

Electron capture of Xe⁵⁴⁺ in collisions with H₂ molecules in the energy range between 5.5 and 30.9 MeV/u

F. M. Kröger^{1,2,3,*} G. Weber,^{1,2} M. O. Herdrich,^{1,2,3} J. Glorius,² C. Langer,⁴ Z. Slavkovská,⁴ L. Bott,⁴ C. Brandau,^{2,5} B. Brückner,⁴ K. Blaum,⁶ X. Chen,⁷ S. Dababneh,⁸ T. Davinson,⁹ P. Erbacher,⁴ S. Fiebiger,⁴ T. Gaßner,² K. Göbel,⁴ M. Groothuis,⁴ A. Gumberidze,² Gy. Gyürky,¹⁰ S. Hagmann,^{2,4} C. Hahn,^{1,2,3} M. Heil,² R. Hess,² R. Hensch,⁴ P. Hillmann,⁴ P.-M. Hillenbrand,² O. Hinrichs,⁴ B. Jurado,¹¹ T. Kausch,⁴ A. Khodaparast,^{2,4} T. Kisselbach,⁴ N. Klapper,⁴ C. Kozhuharov,² D. Kurtulgil,⁴ G. Lane,¹² C. Lederer-Woods,⁹ M. Lestinsky,² S. Litvinov,² Yu. A. Litvinov,² B. Löher,^{2,13} F. Nolden,² N. Petridis,² U. Popp,² M. Reed,¹² R. Reifarh,⁴ M. S. Sanjari,² H. Simon,² U. Spillmann,² M. Steck,² J. Stumm,⁴ T. Szücs,^{10,14} T. T. Nguyen,⁴ A. Taremi Zadeh,⁴ B. Thomas,⁴ S. Yu. Torilov,¹⁵ H. Törnqvist,^{2,13} C. Trageser,^{2,5} S. Trotsenko,² M. Volkmandt,⁴ M. Weigand,⁴ C. Wolf,⁴ P. J. Woods,⁹ V. P. Shevelko,¹⁶ I. Yu. Tolstikhina,¹⁶ and Th. Stöhlker^{1,2,3}

¹Helmholtz-Institut Jena, Jena 07743, Germany

²GSI Helmholtzzentrum für Schwerionenforschung GmbH, Darmstadt 64291, Germany

³Institut für Optik und Quantenelektronik, Friedrich-Schiller-Universität, Jena 07743, Germany

⁴Goethe-Universität, Frankfurt am Main 60323, Germany

⁵Justus-Liebig Universität, Gießen 35390, Germany

⁶Max-Planck-Institut für Kernphysik (MPIK), Heidelberg 69117, Germany

⁷Institute of Modern Physics, Lanzhou 730000, China

⁸Al-Balqa' Applied University, Salt 19117, Jordan

⁹University of Edinburgh, Edinburgh EH8 9YL, United Kingdom

¹⁰Institute for Nuclear Research (Atomki), Debrecen 4001, Hungary

¹¹CENBG, CNRS-IN2P3, Gradignan 33175, France

¹²Australian National University, Canberra 2601, Australia

¹³Technische Universität Darmstadt, Darmstadt 64289, Germany

¹⁴Helmholtz-Zentrum Dresden-Rossendorf (HZDR), Dresden 01328, Germany

¹⁵Saint Petersburg State University, Saint Petersburg 199034, Russia

¹⁶P. N. Lebedev Physical Institute, Moscow 119991, Russia



(Received 19 May 2020; accepted 10 September 2020; published 30 October 2020)

The electron-capture process was studied for Xe⁵⁴⁺ colliding with H₂ molecules at the internal gas target of the Experimental Storage Ring (ESR) at GSI, Darmstadt. Cross-section values for electron capture into excited projectile states were deduced from the observed emission cross section of Lyman radiation, being emitted by the hydrogenlike ions subsequent to the capture of a target electron. The ion beam energy range was varied between 5.5 and 30.9 MeV/u by applying the deceleration mode of the ESR. Thus, electron-capture data were recorded at the intermediate and, in particular, the low-collision-energy regime, well below the beam energy necessary to produce bare xenon ions. The obtained data are found to be in reasonable qualitative agreement with theoretical approaches, while a commonly applied empirical formula significantly overestimates the experimental findings.

DOI: [10.1103/PhysRevA.102.042825](https://doi.org/10.1103/PhysRevA.102.042825)

I. INTRODUCTION

Charge-changing processes, i.e., loss or capture of electrons, occurring in ion-atom and ion-ion collisions belong to the most basic interactions for ion beams. While the theoretical description of projectile ionization of few-electron systems generally leads to reliable results within an uncertainty of

50% for a large range of collision energies and atomic numbers Z [1–3], the rigorous treatment of nonradiative electron capture, i.e., capture where the initial state of the electron cannot be approximated as quasifree, is still a challenging task. This stems from the fact that the process involves a three-body interaction, taking into account the electron of interest and the nuclei of both the projectile and the target, which is difficult to treat theoretically starting from basic principles. Besides basic research, i.e., in atomic and plasma physics as well as astrophysics, the investigation of these processes is motivated by their paramount importance for applications such as the preparation, transport, and storage of highly charged ion beams in accelerator facilities [4–6].

This is particularly evident for the new Facility for Antiproton and Ion Research (FAIR) [7] (currently under construction

*felix.kroeger@uni-jena.de

Published by the American Physical Society under the terms of the [Creative Commons Attribution 4.0 International license](https://creativecommons.org/licenses/by/4.0/). Further distribution of this work must maintain attribution to the author(s) and the published article's title, journal citation, and DOI.

on the campus of the GSI Helmholtzzentrum für Schwerionenforschung), where future studies with heavy, highly charged ions will cover a previously unexplored range of experimental parameters with respect to collision energies, beam intensities, and ion species. An important part of the research program of the Stored Particles Atomic Physics Research Collaboration (SPARC) [8] within the FAIR project concerns studies of highly charged ion beams that are decelerated in the recently commissioned CRYRING@ESR. More specifically, in combination with the Experimental Storage Ring (ESR) as predecelerator, CRYRING@ESR will enable cooling and storage of even the heaviest ions at the highest charge states but at beam energies much below the required (relativistic) production energies for the desired charge states. This is accomplished by deceleration of the ions in the ESR to a typical energy of 10 MeV/u and thereafter injection into CRYRING@ESR. Thus, CRYRING@ESR extends the unique physics potential of the ESR to the low-energy domain (i.e., beam energies from a few MeV/u down to a few 10 keV/u) and will open up various novel research opportunities in the realm of extreme matter research and various neighboring fields [9]. These research activities will profit considerably from the high luminosity of the storage rings combined with the brilliant beams of electron-cooled heavy ions and exotic nuclei.

To name a few examples, due to the low-beam energy (strongly reduced Doppler corrections) it will enable one to improve substantially the accuracy of challenging experiments already pioneered at the ESR such as the $1s$ Lamb shift in H-like heavy ions and the hyperfine-splitting at high atomic numbers Z . Dielectronic recombination studies will profit from the ultracold electron cooler and, in addition, completely new classes of experiments will be opened up. Prominent examples are the study of quasimolecular systems in the critical field regime and the investigation of astrophysical relevant reactions within the (low-energy) Gamow window by using exotic nuclei. In all these experiments, the projectile ions will have charge states much higher than their respective equilibrium charge state, and as a consequence electron capture from the residual gas constituents will be the dominant charge-changing process. In dispersive ion optical elements, the trajectories of ions being up- or down-charged deviate from the one of the reference charge state, resulting in successive defocusing and the eventual partial loss of the ion beam. Modeling these beam losses is of key importance for the efficient planning of experiments. However, experimental electron-capture cross-section data for highly charged ions colliding with atoms and molecules at kinetic energies well below the respective projectile's ionization threshold are to the best of our knowledge basically nonexistent. Therefore, additional experimental data covering a significant range of collision energies as well as ion species and target atoms are needed to benchmark theoretical approaches and scaling laws available for such collision systems.

In this work, cross-section measurements are presented for electron capture into excited states of initially bare xenon (Xe^{54+}) projectiles, occurring in collisions with hydrogen molecules (H_2). This study was conducted using decelerated ion beams in the ESR, thus covering ion beam energies that are relevant for the operation of the CRYRING@ESR. The

obtained electron-capture cross-section data are compared to combined predictions of the radiative electron-capture (REC) and the nonradiative electron-capture (NRC) theories as well as to the widely used empirical Schlachter formula [10].

II. MEASUREMENT TECHNIQUE AND DATA ANALYSIS

During a beam time at the GSI accelerator facility, xenon ions produced in an ion source at low charge states were preaccelerated in the Universal Linear Accelerator (UNILAC) and subsequently injected into the heavy-ion synchrotron SIS18. After being accelerated to a respective beam energy of 100 MeV/u, the ions were ejected into the transfer line from SIS18 to the ESR [11] where all their electrons were removed during the passage through an 11 mg/cm² carbon stripper foil. After injection into the ESR, the ion beam was rebunched and decelerated to the chosen final energies of 5.5, 6, 6.7, 7, 8, 15, and 30.9 MeV/u. This energy range corresponds to relativistic β values from 0.11 to 0.25. Typical beam intensities of several 10^7 particles were stored and electron cooled in order to achieve a good beam quality, resulting in a typical beam diameter in the order of 2 mm as well as a momentum spread in the order of $\Delta p/p \approx 10^{-4}$ [12] after a cooling time of a few seconds. As a next step the internal gas target of the ESR [13,14] was turned on, leading to the formation of a H_2 gas jet with a diameter of about 6 mm [15]. The overlap between the ion beam and the target was optimized based on a scan of the ion beam position through the perpendicular gas jet while monitoring the beam-loss rate. The target area density of 10^{14} particles/cm² was chosen such that charge-changing processes occurring at the intersection point of the gas jet and the ion beam were clearly the dominant beam-loss contribution compared to interactions with the residual gas along the beam line and recombination in the electron cooler. In the energy range of interest, the most relevant charge-exchange processes occurring in ion-atom collisions at the gas target are REC and NRC of a target electron. While for low energies NRC dominates the total capture cross section, it is overtaken by REC with increasing collision energies. By passing through a bending magnet downstream of the gas target, down-charged projectile ions were separated from the reference charge state and subsequently stopped by a multiwire proportional counter (MWPC) [16]. Projectiles decelerated to energies below roughly 10 MeV/u are no longer able to penetrate through the 25- μm stainless steel foil separating the ESR vacuum from the MWPC detector housing. Therefore, the measurement of the electron-capture cross-section had to rely on an indirect technique using an array of three high-purity germanium (HPGe) x-ray detectors that were positioned around the interaction zone of the ion beam and the gas target. Each of these detectors covered a solid angle of about 10^{-2} sr and they were placed with respect to the ion beam axis at 35°, 60°, and at 90° (see Fig. 1 for details).

As an example of the results, in Fig. 2, two x-ray spectra taken at collision energies of 30.9 MeV/u (top panel) and 5.5 MeV/u (bottom panel) at an observation angle of 60° are shown. All relevant features in these spectra can be attributed to either the REC process (i.e., K-REC denotes the radiation emitted by REC into the projectile K shell, L-REC refers to capture into the L shell, and so on) or characteristic

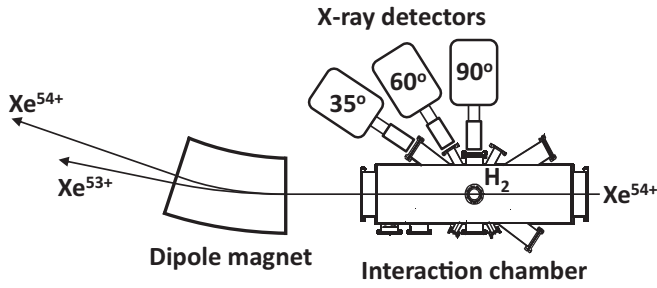


FIG. 1. Schematic drawing of the experimental setup. An array of HPGe x-ray detectors is positioned around the interaction zone of the ion beam and the gas jet target.

K transitions into the ground state ($K\alpha$, $K\beta$, etc.). The difference in the intensity ratios of the REC and the K radiation for both collision energies results from NRC dominating the population of excited projectile states at low collision energies, whereas at the higher energy the REC process prevails. Also visible is an escape peak resulting from the germanium K radiation leaving the detector crystal. All spectra were corrected according to the energy-dependent detection efficiency ε of

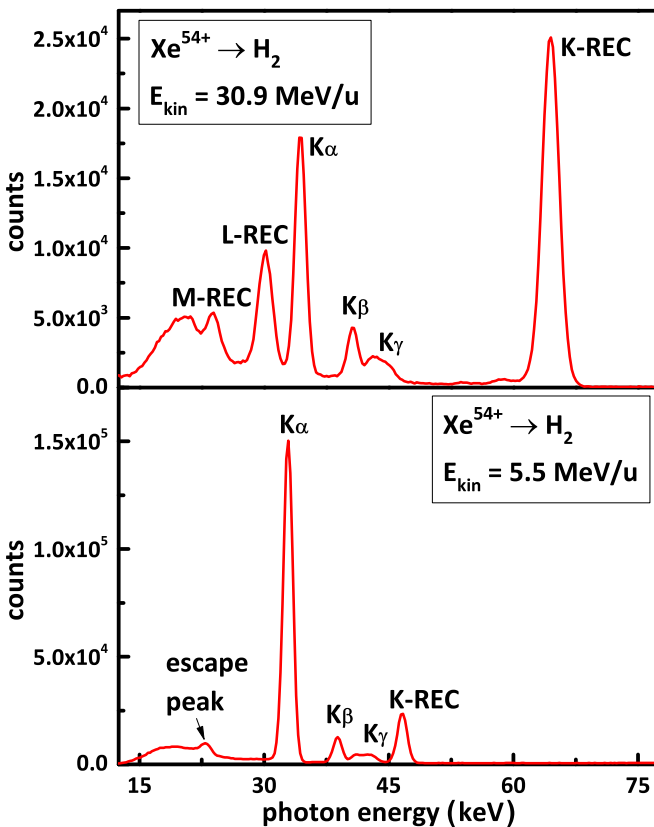


FIG. 2. The x-ray spectra resulting from the collision of bare xenon ions with H₂ gas target, recorded by HPGe x-ray detectors. The spectra were obtained at an observation angle of 60° at the highest and the lowest ion beam energies used in this study. Note that in the laboratory system the peak positions are Doppler shifted with respect to the transition energies in the emitter system. For example the $K\alpha$ energies in the emitter system are close to 30.9 keV ($2s_{1/2} \rightarrow 1s_{1/2}$, as well as $2p_{1/2} \rightarrow 1s_{1/2}$) and 31.3 keV ($2p_{3/2} \rightarrow 1s_{1/2}$).

the respective HPGe detector. The efficiency correction was obtained by modeling the detector response based on the EGS5 Monte Carlo code for photon and electron transport in matter [17]. This code is able to reproduce all relevant features of the detector response as previously demonstrated in Ref. [18].

For a hydrogenlike high- Z system multiphoton transition rates are relatively small compared to single-photon transitions, the most important being the two-photon $2E1$ transition from the $2s_{1/2}$ to the $1s_{1/2}$ state, which has for xenon a rate of about $1.9 \times 10^{11} \text{ s}^{-1}$, while the single-photon $M1$ transition rate between the same states is about $6.3 \times 10^{11} \text{ s}^{-1}$ [19]. Furthermore, in a one-electron system Auger decay of excited states is not possible. As a consequence, for almost all electrons that are captured into excited projectile states the transition to the ground state is accompanied by emission of single-photon K radiation. Therefore, the $K\alpha$, β , γ , ... emission cross section integrated over the complete solid angle is a measure of the electron-capture cross section summed over all principal quantum numbers n , with $n > 1$. A peculiarity of the two spectra in Fig. 2 lies in the increase of the K radiation intensity relative to the REC peaks as the ion beam energy is decreasing. This illustrates the fact that at low beam energies the NRC process is the dominating capture process. Note that in the REC process electrons are most likely captured directly into low- n states, in particular, into the K shell [20]. In contrast, in the NRC process electrons are captured mainly into those projectile states whose momentum distribution has a high overlap with the initial momentum distribution, which is given by the target electrons' intrinsic momentum distribution convoluted and shifted by the relative momentum in the collision [21]. For the present collision parameters this leads predominantly to capture into high- n states, which can be seen in Fig. 2, which subsequently undergo cascades of decays towards the ground state, resulting in intense emission of K radiation.

By normalizing the intensity I_K of the peaks formed by the K radiation to the intensity of the K-REC radiation I_{REC} the K emission cross section σ_K is expressed in terms of the angular differential cross section $d\sigma_{\text{REC}}/d\Omega$ of the REC process as follows:

$$\frac{d\sigma_K}{d\Omega} = \frac{I_K}{I_{\text{REC}}} \frac{\varepsilon_{\text{REC}}}{\varepsilon_K} \frac{d\sigma_{\text{REC}}}{d\Omega}, \quad (1)$$

with ε_K and ε_{REC} being the detector efficiency at the energy of the K radiation and the K-REC radiation, respectively.

A similar normalization procedure to obtain emission cross sections of spectral features relative to the REC peaks has already been used, for example, in Refs. [4,22,23]. It results in a cancellation of sizable sources of uncertainty of the experimental setup such as the solid angle covered by each detector. The necessary K-REC cross-section data, differential in emission angle and photon energy, were produced using the RECAL program [23,24]. This algorithm performs interpolations between precalculated radiative-recombination (RR) differential cross-section values, produced by a code provided by Surzhykov *et al.* [25], and convolutes the resulting data with the tabulated Compton profile of the target atom [26]. The reduction of the REC process to the RR process, which in turn can conveniently be described as the time-inverse process of photoionization, is justified as long as the target

electrons' initial binding energy and momentum distribution are negligible compared to the energy and momentum transfer during the capture process; i.e., the initial electron can be treated as quasifree. This requirement is fulfilled in the present case of a strongly asymmetric collision system, thus enabling the approximation of the REC process as the time inverse of the well-understood photoionization process (see Ref. [20] for details). In the aforementioned code the photoionization cross section is obtained within the framework of the Dirac theory for bound and free states, while assuming a pointlike nucleus, and by making use of the partial-wave expansion of the continuum electron wave function. The coupling to the electromagnetic radiation is treated within the framework of the first-order perturbation theory. In order to compute all the angular differential properties, moreover, the density matrix theory is applied. Based on this approach the K-REC differential cross section is expected to be predicted with an accuracy of a few percent [27]. On the other hand, basically all measurements of the absolute REC cross section reported in the literature exhibit uncertainties in the range of 20% to 50% [20,28], thus limiting the experimental verification of any theoretical treatment to this level. In general, an accurate experimental determination of absolute cross-section values is challenging since target densities, absolute beam intensities, and beam-target overlap have to be determined precisely and also a detailed knowledge of the outgoing particle detection efficiency is required.

However, because the underlying process of photoionization is believed to be well understood and because for the present case the aforescribed approximation of a quasifree incident electron is valid, there should be no reason why the predicted K-REC (or equivalently K-RR into a bare ion) cross section should not be accurate to a few percent. Especially since for the present collision system, there is basically no difference between the nonrelativistic and relativistic predictions when it comes to the differential cross sections. This increases the confidence that no significant effects are missing in the theory (QED effects can be basically neglected at this level of accuracy). Moreover, this technique of normalizing on REC/RR has been already successfully used in previous studies at storage rings (e.g., Ref. [4]). In addition, it should be emphasized that for the determination of x-ray emission cross sections, the normalization of experimental data to radiative recombination transitions is a well-established method at electron beam ion traps [29,30].

In the emitter system the angular differential cross section of an electric dipole transition is linked to the total transition cross section from the initial to the final state $\sigma_{E1}^{i \rightarrow f}$ by [31]

$$\frac{d\sigma_{E1}}{d\Omega} = \frac{\sigma_{E1}^{i \rightarrow f}}{4\pi} [1 + \beta^{\text{eff}} A (1 - 3/2 \sin^2 \theta)], \quad (2)$$

where β^{eff} is the so-called effective anisotropy parameter that is nonzero for transitions from initial states with angular quantum numbers $j > 1/2$ and A is the alignment parameter that takes a nonzero value if the initial state exhibits a nonstatistical population of the magnetic substates. Note that a nonstatistical population is a common feature of excited states of highly charged ions produced in collision processes, such as REC [32] and NRC [33]. We adjusted Eq. (2) to the

experimental $d\sigma_K/d\Omega$ data points by treating the total cross section and the product $\beta^{\text{eff}} A$ as free parameters, while taking into account the relativistic transformation of the observation angle and the solid state element from the laboratory to the emission system. As mentioned above, the overwhelming majority of electrons captured to excited states of the projectile will decay to the ground state with the emission of K radiation. Thus, the obtained K emission cross section is in good approximation equal to the total electron-capture cross section for all projectile states with $n > 1$. However, for some energies only spectral data from the detectors at 60° and 90° were available. These observation angles are too close to each other to extract the underlying angular distribution in a meaningful way. Nevertheless the angular distribution where all three detector positions are available exhibits only a small degree of anisotropy. In fact, all obtained anisotropy parameters are within 1σ compatible with zero. This is also expected from first principles as the anisotropic $2p_{3/2} \rightarrow 1s_{1/2}$ transition is superimposed by the isotropic $2p_{1/2}, 2s_{1/2} \rightarrow 1s_{1/2}$ transitions and also the alignment of the $2p_{3/2}$ state by direct population is subsequently diluted by cascade feeding. Thus, where the experimental data were limited to two observation angles we approximated the total cross section by averaging the angular-dependent emission cross sections measured by both detectors, implicitly assuming an isotropic emission pattern. A conservative estimate of the overall uncertainty including systematics (the detector efficiency) of the obtained total emission cross section for all collision energies amounts to $\pm 10\%$, assuming that the theoretical K-REC cross section is accurate to a few percent.

III. THEORETICAL APPROACHES FOR ELECTRON CAPTURE

In the following, various theoretical methods available for cross-section calculations for the processes of radiative and nonradiative electron capture from low- Z targets by heavy projectiles are briefly described. In addition the Schlachter formula, which yields an empirical estimate of the total cross section for electron capture based on a set of experimental data that was available in the early 1980s, is presented. All these approaches are then compared to the experimental results. It should be noted that a variety of other methods for the treatment of the nonradiative electron-capture process exists, e.g., n -particle classical trajectory Monte Carlo simulations, continuum distorted wave theory, and coupled channel method, just to name a few. However, in this work we take into account only those treatments that are readily available and frequently used within the community for prompt and pragmatic estimates of charge-exchange rates and ion beam lifetimes.

Radiative electron capture. The cross section for electron capture, due to the REC process integrated over all photon emission angles, was obtained by two separate methods. To obtain the cross sections for capture into projectile shells with principle quantum numbers $n = 2$ and 3 , an interpolation was performed on an extensive tabulation of cross-section values published by Ichihara and Eichler [34]. These values are based on fully relativistic calculations which also include

the effects of the finite nuclear size and all multipole orders of the photon field for RR into the K, L, and M shells of bare ions. The only difference between this approach and the one on which the RECAL code is based is the consideration of the finite nuclear size in the former. Therefore, the cross sections from Ichihara and Eichler [34] can be considered to be more complete in principle. However, for the present level of accuracy the difference is not significant. Moreover, for the shells $n > 3$ a nonrelativistic approach was used which is generally applicable when both the collision energy and the binding energy of the captured electron are considerably smaller than the electron rest mass. This treatment of the RR process is based on recurrence relations as described in Ref. [20].

Nonradiative electron capture according to the eikonal approximation. The eikonal approximation is known to describe total electron-capture cross sections for asymmetric collision systems at high energies within a factor of 2 to 3. Within the eikonal approximation, one center is treated in first-order $Z\alpha$, whereas the other center is described nonperturbatively. A closed formula for the relativistic eikonal approximation of electron capture from the $1s$ state of a hydrogenlike target into the $1s$ shell of an initially bare projectile was derived by Eichler [35]. It has the form

$$\sigma_{1s,1s}^{\text{eik}} = a_0^2 \pi \frac{2^8 (Z_p Z_T)^5}{5v^2 (Z_T^2 + p_-^2)^5} \frac{1 + \gamma}{2\gamma^2} \frac{\pi \eta Z_T'}{\sinh(\pi \eta Z_T')} \times e^{-2\eta Z_T \tan^{-1}(-p_-/Z_T)} (S_{\text{eik}} + S_{\text{magn}} + S_{\text{orb}}), \quad (3)$$

where Z_p and Z_T denote the atomic numbers of the projectile and the target, respectively; v is the collision velocity; γ is the associated relativistic Lorentz factor; and a_0 denotes the Bohr radius. For a detailed explanation of the other parameters in Eq. (3) the reader is referred to the original publication [35]. The parameter Z_T' , which in the present work was chosen as $Z_T' = Z_T$, represents the potential of the target system in a final-state interaction with the captured electron now being bound to the projectile. For the present case, where the projectile potential is the stronger one, the “post” version of the eikonal approximation was adopted by exchanging $Z_p \leftrightarrow Z_T$ and substituting Z_T' with Z_p' . It was shown by Meyerhof *et al.* [36] that the eikonal cross section averaged over a complete principal shell scales with Z/n for initial and final states, thus enabling the extension of Eq. (3) to capture from and into shells having arbitrary quantum numbers n by making the substitutions $Z_T \rightarrow Z_T/n_T$ and $Z_p \rightarrow Z_p/n_p$, respectively. For practical purposes a cutoff value is necessary for the highest projectile shells to be considered, which in this work was set to $n_{\text{cut}} = 50$. It should be noted that the underlying approximations for the closed formula presented by Eichler are only valid for collision velocities higher than the orbital velocities of the initial and the final state of the electron, which is for most collision energies under investigation clearly not the case with respect to the projectile K and L shells. However, as the total NRC cross section is dominated by capture into those shells that have the largest overlap with the initial electron momentum distribution (taking into account the collision velocity), the contribution by capture into the K and L shells is rather small at the relatively low collision energies which are of interest in this work.

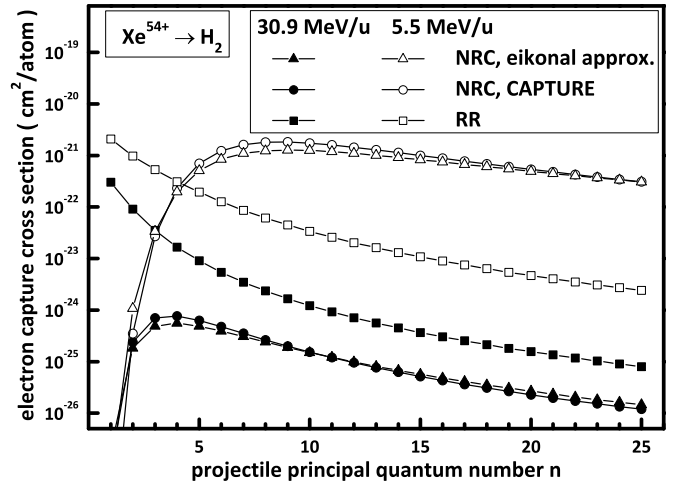


FIG. 3. Theoretical electron-capture cross sections against the projectile principle quantum number n for the collision of Xe⁵⁴⁺ with a H₂ target at kinetic beam energies of 5.5 and 30.9 MeV/u. The cross sections are given per target molecule constituent, i.e., per atom. The RR cross-section data were produced with a nonrelativistic treatment based on recurrence relations, while the NRC cross-section values were calculated using the eikonal approximation as well as the CAPTURE code. It is found that both NRC treatments yield very similar results, with the CAPTURE code predicting cross-section values slightly larger than those of the eikonal approximation.

Nonradiative electron capture according to the CAPTURE code. This code is based on the normalized Brinkman-Kramers (NBK) approximation in the impact parameter representation [37,38]. Like the eikonal approximation it utilizes hydrogenlike radial wave functions to describe the initial and the final state of the captured electron. The total NRC cross section is given as a sum of partial cross sections σ_{n^f, n^i} for capture from all occupied target electron shells with the principle quantum number n^i into all possible final projectile states having the principal quantum number n^f as follows:

$$\sigma^{\text{CAPTURE}} = \sum_{n^f=1}^{n_{\text{cut}}^f} \sum_{n^i=1}^{n_{\text{max}}^i} \sigma_{n^f, n^i},$$

$$\sigma_{n^f, n^i} = 2\pi \int_0^{b_{\text{max}}} P_{n^f, n^i}^{\text{norm}}(b) b db,$$

$$P_{n^f, n^i}^{\text{norm}}(b) = \frac{P_{n^f, n^i}(b)}{1 + \sum_{n' \neq n^f} P_{n', n^i}(b)}, \quad (4)$$

where $P_{n^f, n^i}(b)$ is the probability according to the Brinkman-Kramers (BK) treatment for capture of an electron from the (initial) target shell n^i into the (final) projectile shell n^f , depending on the impact parameter b . The main feature of this approach is that the normalized capture probability P^{norm} is always less than unity, making it possible to use the NBK approximation even at lower energies which are not accessible with the pure BK approximation.

In Fig. 3 electron-capture cross sections are presented which result from the aforementioned treatments for the collision of bare xenon projectiles with hydrogen at the lowest and at the highest collision energy under investigation in this work. As can be seen both NRC treatments predict very similar cross

TABLE I. Experimental electron-capture cross-section data obtained in this work in comparison with the sum of predictions for the NRC and the REC process, as presented in Fig. 4(a), assuming that the theoretical K-REC cross section used for normalization is accurate to a few percent. The stated uncertainties reflect the experimental contribution only and do not account for potential theoretical uncertainties in the prediction of the K-REC cross section that was used for normalization (see text for details).

Collision system	Collision energy (MeV/u)	Electron capture into $n > 1$ (10^3 barn/atom)	
		Experiment	NRC + REC
$\text{Xe}^{54+} \rightarrow \text{H}_2$	5.5	14.9 ± 1.49	22.3
	6	10.6 ± 1.06	15.1
	6.7	7.2 ± 0.72	9.4
	7	6.1 ± 0.61	7.9
	8	3.7 ± 0.37	4.6
	15	0.73 ± 0.07	0.74
	30.9	0.17 ± 0.02	0.19

sections, with the CAPTURE code predicting values slightly larger than those of the eikonal approximation. In fact, it is known that setting $Z' = 0$ in the eikonal approximation results in a capture cross section identical to the NBK value [35]. While the RR/REC process is dominated by the capture into low- n states of the projectile, the NRC process exhibits the largest cross section for capture into those shells having the largest overlap with the initial electron momentum distribution. Since hydrogen has a very narrow intrinsic momentum distribution, the initial electron momentum is effectively defined by the collision velocity. As a consequence, the NRC cross section peaks at principal quantum numbers of the projectile that roughly correspond to orbital velocities around half the collision velocity. Thus, for probing the predictive power of NRC treatments in the context of the present work, it is reasonable to focus on capture into excited states and to neglect the contribution of the K shell. The theoretical data integrated over electron capture into all projectile principle quantum numbers $n \geq 2$ are presented in Fig. 4(a), as described in Sec. IV.

Total electron capture according to the Schlachter formula. An empirical cross-section formula for single-electron capture was obtained by Schlachter *et al.* [10] based on a large data set covering collision energies between 0.3 and 8.5 MeV/u and initial projectile charge states up to 59+. This so-called Schlachter formula has the following form:

$$\sigma_{\text{Schlachter}} = \frac{q^{0.5}}{Z_T^{1.8}} \frac{1.1 \times 10^{-8}}{\tilde{E}^{4.8}} (1 - e^{-0.037\tilde{E}^{2.2}}) \times (1 - e^{-2.44 \times 10^{-5} \tilde{E}^{2.6}}) [\text{cm}^2/\text{atom}], \quad (5)$$

where q denotes the projectile charge and the reduced energy $\tilde{E} = E/(Z_T^{1.25} q^{0.7})$ is derived from the kinetic projectile energy E expressed in units of keV/u. The range of validity is stated as $q \geq 3$ and $10 \leq \tilde{E} < 1000$. The underlying data do not contain highly charged, heavy projectiles with open K and L shells at collision velocities, where the REC process significantly contributes to the total capture cross section.

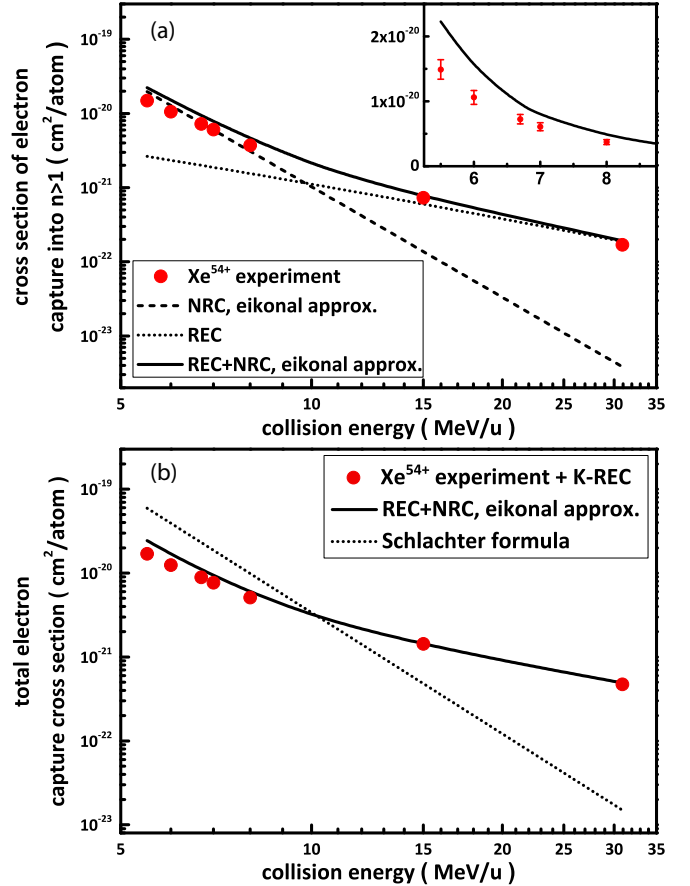


FIG. 4. (a) Cross section of electron capture from hydrogen into excited states of xenon projectiles as a function of the collision energy. The experimental data are shown together with theoretical cross sections for the REC and the NRC process. The inset plot has a linear scaling and shows the systematic overestimation at lower beam energies where the NRC process dominates in more detail, together with the experimental uncertainties as stated in Table I. (b) Total electron-capture cross section, produced by amending both the experimental and the theoretical data for capture into excited projectile states with the theoretical K-REC cross section. As can be seen, the Schlachter formula is unable to reproduce the experimental data at both low collision and high collision energies.

This is the reason why, even though the conditions for q and \tilde{E} are fulfilled (with the exception of the 30.9 MeV/u data point which corresponds to $\tilde{E} = 1900$), the applicability of the Schlachter formula is questionable for the collision system addressed in this work. However, as the Schlachter formula is widely used for pragmatic estimations of the capture cross section in ion-atom collisions, it is important to test its predictive power in a variety of scenarios including also edge cases like the mentioned ones [see the Fig. 4(b)].

IV. RESULTS AND DISCUSSION

The experimental cross-section values obtained in this work for electron capture into excited projectile states are presented in Fig. 4(a). For the 15 and 30.9 MeV/u data points, where the REC contribution to the total capture cross section is dominant, a correction for the unobserved capture events

due to two-photon decay from the $2s_{1/2}$ state was applied. Taking into account the direct population by the REC process as well as cascade feeding from all other states with $n = 2$ and 3 results in an enhancement of the electron-capture cross section by 3.4% and 5.5%, respectively. For the lower beam energies, a correction is not necessary as the NRC process, in contrast to the REC process, is only sparsely populating the $2s_{1/2}$ state. Also shown in Fig. 4(a) are theoretical cross sections for the REC and the NRC process. For the latter only the eikonal approximation is shown as the CAPTURE code yields cross-section values that are very similar, as can be seen in Fig. 3, so that both data sets would be hardly distinguishable. The depicted cross-section values are also listed in Table I. For the energy region that is not completely dominated by the REC process, it is found that both NRC treatments lead to a systematic overestimation of the experimental data while reproducing the overall shape of the cross section fairly well. As the eikonal approximation yields slightly smaller values it is in marginally better agreement with the experimental results. Nevertheless, a deviation from the experimental findings by 25% to 50% is observed, with an increasing trend at lower beam energies. This feature is shown in more detail in the inset plot of Fig. 4(a).

As far as the operation of storage rings like CRYRING@ESR is concerned, the most relevant information on electron capture is the total cross section integrated over capture into all projectile states. It allows the estimation of important beam parameters, such as beam losses caused by charge-exchange processes, making it a crucial input for the planning of future experiments and the design of experimental setups. In Fig. 4(b) total electron-capture cross sections are presented. These were obtained by adding the theoretical K-REC cross section (interpolated from the tabulated values by Ichihara and Eichler [34]) to the experimental data and also to the theoretical capture cross sections into projectile states with $n > 1$. It should be noted that for all collision energies considered in this study NRC into the K shell is negligible, whereas REC into the K shell is the dominant REC contribution, as can be seen in Fig. 3.

From a practical point of view the comparison shown in Fig. 4(b) is the most relevant to assess the predictive power of the various treatments for electron capture. As can be seen, in the lower-energy region where NRC is the dominating capture process, once again the REC + NRC capture cross section is systematically larger by up to 50% when compared to the experimental values. Nevertheless, when taking into account the experimental uncertainties, there is a reasonable qualitative agreement overall. In contrast, the Schlachter formula fails to reproduce the REC contribution which results in a severe underestimation of the total capture cross section on the high-energy part of the data set, while it significantly overestimates the capture cross section at lower energies, where NRC dominates. More specifically, the Schlachter formula exhibits an energy dependence similar to that predicted by the eikonal approximation and the CAPTURE code, but yields absolute values that are roughly by a factor of 3 larger, which is clearly in disagreement with the experimental data. At first glance, the apparent inapplicability of the empirical formula in this study is not surprising since the underlying data set does not contain heavy, highly charged ions with open K and

L shells such as bare xenon. This explains why the REC contribution is not reproduced well by the Schlachter formula. However, in contrast to the REC process, these open inner shells of the projectile do not contribute significantly to the total NRC cross section in the energy range under investigation. Thus, it is notable that a large deviation is also found in the NRC-dominated energy region. We also note that for the lowest two energies the total cross section exceeds 0.1 Mb. This implies large capture probabilities as a function of the impact parameter. Under such conditions we would expect that taking into account electron and target ionization in addition in a coherent fashion would be a more appropriate way to treat the collision system under discussion. Therefore we would expect that coupled-channel calculations would be a promising approach to improve the prediction power of the theory.

In this context it is also worth noting that in a previous electron-capture study using decelerated highly charged ions, namely, hydrogenlike germanium in collision with a neon target, good agreement with the Schlachter formula was found [39]. In that study the experimental data were also well reproduced by an n -particle classical trajectory Monte Carlo calculation. In contrast, the eikonal approach resulted in an overestimation of the capture cross section by about a factor of 2. However, one has to keep in mind that germanium ions colliding with neon atoms is a significantly more symmetric collision system than xenon colliding with hydrogen which was studied in the present case. Summarizing, given the range of relevant collision parameters, further experimental studies of cross-section data for electron capture by highly charged, medium to high- Z ions at low collision energies are necessary to draw definite conclusions on the reliability and range of applicability of the various theoretical and empirical predictions.

V. SUMMARY AND OUTLOOK

The cross section for electron capture into excited projectile states was measured in collisions of Xe⁵⁴⁺ with a H₂ target in a low-energy regime not accessible up to now. At such low velocities highly charged heavy ions have charge states much higher than their respective equilibrium charge state, and as a consequence electron capture from the residual gas constituents is the dominant beam-loss process. Thus, precise knowledge of electron-capture cross sections is crucial for the correct estimation of charge-exchange rates and ion beam lifetimes in accelerators and storage rings. The obtained cross-section values were compared to theoretical treatments of the nonradiative capture and the radiative electron capture, as well as an empirical formula for total electron capture. It is found that nonradiative electron-capture cross-section values predicted by the eikonal approximation and the CAPTURE code are in reasonable qualitative agreement with the experimental findings, even though with decreasing beam energy the electron capture is overestimated by up to 50%. This still reasonable agreement is quite remarkable considering that both theories applied are high-energy approximations. For the current beam energy regime and even lower energies, it is evident that more adequate low-energy models need to be investigated and applied. Moreover, the commonly used empirical Schlachter formula significantly overestimates the

total capture cross section at low collision energies, where nonradiative capture dominates.

ACKNOWLEDGMENTS

This project has received funding from the European Research Council (ERC) under the European Union's Horizon 2020 research and innovation programme (Grant No. 682841 "ASTRUM"). Moreover, this work was supported by the Helmholtz International Center for FAIR (HIC for FAIR), by the Bundesministerium für Bildung und Forschung (BMBF) (Grants No. 05P15RFFAA and No. 05P15RGFAA), by the Science and Technology Facilities Council (STFC) UK (Grants No. ST/L005824/1, No. ST/M001652/1, and No. ST/M006085), by the Helmholtz-CAS Joint Research

Group (Grant No. HCJRG-108), and by the Helmholtz-OCPC Postdoctoral Program 2017 (Grant No. GSI08). F.M.K. acknowledges support by the BMBF Verbundprojekt 05P2018 (Grant No. ErUM-FSP T05). C.L.W. acknowledges support by the European Research Council (Grant No. ERC-2015-StG Nr. 677497 "DoRES"). S.D. gratefully acknowledges the support provided by the Alexander von Humboldt Foundation and the Jordanian Scientific Research Support Fund under Grant No. Bas/2/4/2014. S.Yu.T. acknowledges the support by the DAAD through a Mendeleev grant, SPbU (Grant No. 28999675). Yu.A.L. acknowledges the support by the DAAD through Programm des Projektbezogenen Personenaustauschs (PPP) with China [Project ID 57389367]. T.S. acknowledges support from the Helmholtz Association (Grant No. ERC-RA-0016).

-
- [1] R. Anholt, W. E. Meyerhof, X.-Y. Xu, H. Gould, B. Feinberg, R. J. McDonald, H. E. Wegner, and P. Thieberger, *Phys. Rev. A* **36**, 1586 (1987).
- [2] Th. Stöhlker, D. Ionescu, P. Rymuza, T. Ludziejewski, P. Mokler, C. Scheidenberger, F. Bosch, B. Franzke, H. Geissel, O. Klepper *et al.*, *Nucl. Instrum. Methods Phys. Res., Sect. B* **124**, 160 (1997).
- [3] A. B. Voitkiv, B. Najjari, and J. Ullrich, *Phys. Rev. A* **76**, 022709 (2007).
- [4] Th. Stöhlker, T. Ludziejewski, H. Reich, F. Bosch, R. W. Dunford, J. Eichler, B. Franzke, C. Kozhuharov, G. Menzel, P. Mokler, F. Nolden, P. Rymuza, Z. Stachura, M. Steck, P. Swiat, A. Warczak, and T. Winkler, *Phys. Rev. A* **58**, 2043 (1998).
- [5] V. P. Shevelko, M. S. Litsarev, Th. Stöhlker, H. Tawara, I. Y. Tolstikhina, and G. Weber, in *Atomic Processes in Basic and Applied Physics*, edited by V. Shevelko and H. Tawara (Springer, Berlin, 2012), p. 125.
- [6] H. Imao, H. Okuno, H. Kuboki, S. Yokouchi, N. Fukunishi, O. Kamigaito, H. Hasebe, T. Watanabe, Y. Watanabe, M. Kase *et al.*, *Phys. Rev. Spec. Top.—Accel. Beams* **15**, 123501 (2012).
- [7] V. E. Fortov, B. Y. Sharkov, and H. Stöcker, *Phys.-Usp.* **55**, 582 (2012).
- [8] Th. Stöhlker, Yu. A. Litvinov, A. Bräuning-Demian, M. Lestinsky, F. Herfurth, R. Maier, D. Prasuhn, R. Schuch, and M. Steck, *Hyperfine Interact.* **227**, 45 (2014).
- [9] M. Lestinsky, V. Andrianov, B. Aurand, V. Bagnoud, D. Bernhardt, H. Beyer, S. Bishop, K. Blaum, A. Bleile, A. Borovik *et al.*, *Eur. Phys. J.: Spec. Top.* **225**, 797 (2016).
- [10] A. S. Schlachter, J. W. Stearns, W. G. Graham, K. H. Berkner, R. V. Pyle, and J. A. Tanis, *Phys. Rev. A* **27**, 3372 (1983).
- [11] B. Franzke, *Nucl. Instrum. Methods Phys. Res., Sect. B* **24–25**, 18 (1987).
- [12] M. Steck, P. Beller, K. Beckert, B. Franzke, and F. Nolden, *Nucl. Instrum. Methods Phys. Res., Sect. A* **532**, 357 (2004).
- [13] R. E. Grisenti, R. A. C. Fraga, N. Petridis, R. Dörner, and J. Deppe, *Europhys. Lett.* **73**, 540 (2006).
- [14] M. Kühnel, N. Petridis, D. Winters, U. Popp, R. Dörner, Th. Stöhlker, and R. Grisenti, *Nucl. Instrum. Methods Phys. Res., Sect. A* **602**, 311 (2009).
- [15] T. Gassner and H. F. Beyer, *Phys. Scr.*, **T166**, 014052 (2015).
- [16] O. Klepper and C. Kozhuharov, *Nucl. Instrum. Methods Phys. Res., Sect. B* **204**, 553 (2003).
- [17] H. Hirayama, Y. Namito, A. F. Bielajew, S. J. Wilderman, and W. R. Nelson, *The EGS5 Code System, Report SLAC-R-730*, (Stanford Linear Accelerator Center, California, USA, 2005).
- [18] G. Weber, H. Bräuning, R. Martin, U. Spillmann, and Th. Stöhlker, *Phys. Scr.*, **T144**, 014034 (2011).
- [19] A. Volotka (personal communication) (2019).
- [20] J. Eichler and Th. Stöhlker, *Phys. Rep.* **439**, 1 (2007).
- [21] A. Ichihara, T. Shirai, and J. Eichler, *Phys. Rev. A* **49**, 1875 (1994).
- [22] T. Ludziejewski, Th. Stöhlker, S. Keller, H. Beyer, F. Bosch, O. Brinzarescu, R. W. Dunford, B. Franzke, C. Kozhuharov, D. Liesen *et al.*, *J. Phys. B: At., Mol. Opt. Phys.* **31**, 2601 (1998).
- [23] M. Herdrich, G. Weber, A. Gumberidze, Z. Wu, and Th. Stöhlker, *Nucl. Instrum. Methods Phys. Res., Sect. B* **408**, 294 (2017).
- [24] G. Weber, H. Ding, M. O. Herdrich, and A. Surzhykov, *J. Phys.: Conf. Ser.* **599**, 012040 (2015).
- [25] A. Surzhykov, S. Fritzsche, and Th. Stöhlker, *Phys. Lett. A* **289**, 213 (2001).
- [26] F. Biggs, L. Mendelsohn, and J. Mann, *At. Data Nucl. Data Tables* **16**, 201 (1975).
- [27] A. Surzhykov (personal communication) (2020).
- [28] Th. Stöhlker, C. Kozhuharov, P. H. Mokler, A. Warczak, F. Bosch, H. Geissel, R. Moshhammer, C. Scheidenberger, J. Eichler, A. Ichihara *et al.*, *Phys. Rev. A* **51**, 2098 (1995).
- [29] R. E. Marrs, S. R. Elliott, and D. A. Knapp, *Phys. Rev. Lett.* **72**, 4082 (1994).
- [30] K. R. Brown, R. J. Clark, J. Labaziewicz, P. Richerme, D. R. Leibbrandt, and I. L. Chuang, *Phys. Rev. A* **75**, 015401 (2007).
- [31] A. Surzhykov, U. D. Jentschura, Th. Stöhlker, and S. Fritzsche, *Phys. Rev. A* **73**, 032716 (2006).
- [32] Th. Stöhlker, F. Bosch, A. Gallus, C. Kozhuharov, G. Menzel, P. H. Mokler, H. T. Prinz, J. Eichler, A. Ichihara, T. Shirai *et al.*, *Phys. Rev. Lett.* **79**, 3270 (1997).
- [33] J. P. Hansen, L. Kocbach, A. Dubois, and S. E. Nielsen, *Phys. Rev. Lett.* **64**, 2491 (1990).
- [34] A. Ichihara and J. Eichler, *At. Data Nucl. Data Tables* **74**, 1 (2000).

- [35] J. Eichler, *Phys. Rev. A* **32**, 112 (1985).
- [36] W. E. Meyerhof, R. Anholt, J. Eichler, H. Gould, C. Munger, J. Alonso, P. Thieberger, and H. E. Wegner, *Phys. Rev. A* **32**, 3291 (1985).
- [37] V. P. Shevelko, *Tech. Phys.* **46**, 1225 (2001).
- [38] V. P. Shevelko, O. Rosmej, H. Tawara, and I. Y. Tolstikhina, *J. Phys. B: At., Mol. Opt. Phys.* **37**, 201 (2004).
- [39] Th. Stöhlker, C. Kozhuharov, P. H. Mokler, R. E. Olson, Z. Stachura, and A. Warczak, *J. Phys. B: At., Mol. Opt. Phys.* **25**, 4527 (1992).